

**Javier A. ORTEGA-SÁENZ\***, **Marco A.L. HERNANDEZ-RODRIGUEZ\***, **Remigiusz MICHALCZEWSKI\*\***,  
**Jerzy SMOLIK\*\***, **Marian SZCZEREK\*\***

## **THE MECHANICAL PROPERTIES OF PVD COATINGS DEPOSITED ON NITRIDED CoCrMo ALLOY**

## **WŁAŚCIWOŚCI MECHANICZNE POWŁOK PVD OSADZANYCH NA AZOTOWANYM STOPIE CoCrMo**

### **Key words:**

CoCrMo alloy, nitriding, PVD coatings

### **Słowa kluczowe:**

stop CoCrMo, azotowanie, powłoka PVD

### **Summary**

The paper concerns the evaluation of mechanical properties of the composite: ‘nitrided layer-PAPVD coating’ created on CoCrMo alloy intended for biotribological applications.

---

\* Universidad Autónoma de Nuevo León, FIME-CIDIIT, Av. Universidad S/N, San Nicolás de los Garza, Nuevo León 66450, México.

\*\* Institute for Sustainable Technologies – National Research Institute, ul. K. Pułaskiego 6/10, 26-600 Radom, Poland.

Five nitriding processes with varying nitriding potential ( $p(N_2/H_2) = 1.0, 1.5, 2.0, 2.5$  and  $3.0$ ) were selected for optimising. The modulus of elasticity and nanohardness of nitrided layers were measured by nanoindentation. Cross-sections were examined by means of scanning electron microscopy (SEM) in order to determine the thickness and the uniformity of the affected zone after nitriding. The change in surface roughness was studied with the help of 3D roughness parameters obtained by atomic force microscopy (AFM) and the phase composition was determined by means of X-ray diffraction (XRD). It was found that the most suitable properties of the surface layer were achieved by nitriding at  $p(N_2/H_2) = 2.5$ .

CrN as well as multilayer (TiN/CrN) $\times$ 3 PAPVD coatings were deposited onto the substrates with and without nitriding for evaluation of the nitriding effect on the adhesion. CoCrMo alloy nitrided sample was included for comparison. All these conditions were characterised by means of AFM, nanohardness, SEM, and scratch test.

The duplex technology applied to CoCrMo orthopaedic alloy allows for a significant increase of the adhesion of the PAPVD coatings and the improvement of the load carrying capacity of the CoCrMo orthopaedic alloy.

## INTRODUCTION

Premature wear is the main cause of orthopedic implants failure. Co-CrMo alloy is one of the most used metallic biomaterials due to its high resistance to wear and corrosion. However, the toxicity of metallic ions of Co and Cr ions released from wear particles into the human body is a concern which has motivated to looking for alternatives to solve or diminish this problem. Plasma nitriding of alloy forged CoCrMo is an alternative that has been previously studied [L. 1–3] and it has shown an improvement in the mechanical properties and also wear and fatigue resistance of the CoCrMo alloy. Another option previously studied has been the application of PVD and CVD coatings to hip joint replacements [L. 4, 5], which has revealed promising results. Nevertheless, the combination of these two techniques, known as duplex treatment, is another alternative that can be studied for orthopedic materials like CoCrMo alloy. Moreover, it has been reported that the nitrided substrate improves the adhesion of coatings [L. 6–11].

The aims of the present study were to analyze the nitriding behaviour of forged CoCrMo alloy and determine if it is possible to improve the adhesion of PAPVD coatings to alloy by nitriding process. To achieve the first objective, five nitriding processes with different nitriding potential were executed and samples characterized. An optimal nitriding potential was selected to create duplex composites (PAPVD + nitriding) using two different PAPVD coatings: monolayer CrN and multilayer (TiN/CrN) $\times$ 3. Structural and mechanical properties of the five nitriding samples and those of duplex composites were determined by means of several analytical methods. Scratch tests were done to PAPVD coatings in forged CoCrMo alloy samples with and without previous nitriding to accomplish the second aim of this study. Results from duplex coated specimens were compared to results from CoCrMo nitrided and PAPVD coated but not nitrided specimens in order to extract the contributions of the nitriding process and the hard ceramic coating.

## EXPERIMENTAL DETAILS

### Preparation of the composites

For the experiments, medical grade forged CoCrMo alloy (ASTM 1537) with a chemical composition of 28% Cr, 5.88% Mo, 1.18% Si, 0.13% Ni, 0.15% Fe, 0.06% C (wt. %) and balance Co (wt%) was used. Samples of 30 mm diameter with 6 mm thickness were ground and polished to obtain mirrorlike smoothness ( $R_a = 0.01 \mu\text{m}$ ).

Five experimental nitriding processes were performed using five different nitriding potentials ( $p(\text{N}_2/\text{H}_2) = 1.0, 1.5, 2.0, 2.5$  and  $3.0$ ) in forged CoCrMo alloy samples to select the optimal nitriding potential. Nitriding processes were carried out in plasma assisted physical vapour deposition device (Standard 1) at a temperature of  $520^\circ\text{C}$ , for a time of 7 hours using prescribed nitriding potentials. The optimal nitriding potential was selected according to parameters such as thickness of the nitrided layer, roughness, hardness and Young's modulus. Once nitriding potential was selected, duplex composites (nitrided layer/PAPVD coating) were created by means of the duplex surface treatment method in a two-stage separable cycle (first the nitriding process and then the PAPVD coating deposition). The PAPVD coating deposition was executed by means of the assisted physical vapour deposition device (Standard 1). Two different PVD coatings were deposited: monolayer CrN and multilayer

(TiN/CrN)×3. Samples of forged CoCrMo alloy without previous nitriding were also coated. Parameters of the duplex processes are presented in **Table 1**.

**Table 1. Parameters of the duplex treatment technology**

Tabela 1. Parametry technologii duplex

<i>Stage-1: Gas Nitriding</i>						
Temperature (°C)	Atmosphere		Nitriding potential	po-	Time (min)	
520	11.1%N <sub>2</sub> + 88.9% H <sub>2</sub>		2.5		420	
<i>Stage-2: PAPVD coating deposition</i>						
Coating	Particular layer	Atmosphere	Preassure (MPa)	Temperature (°C)	Ubias (V)	Time (min)
Multilayer (TiN/CrN)×3	TiN	N <sub>2</sub>	1.2 × 10 <sup>-6</sup>	400	-200	30
	CrN	N <sub>2</sub>	3.5 × 10 <sup>-6</sup>	400	-200	30
Monolayer CrN	CrN	N <sub>2</sub>	3.5 × 10 <sup>-6</sup>	400	-200	120

Five different types of surface treatments were obtained by using previously described procedures: (1) nitrided CoCrMo, (2) CoCrMo with CrN monolayer (plain CrN), (3) nitrided CoCrMo with CrN monolayer (CrN duplex), (4) CoCrMo with (TiN/CrN)×3 multilayer (plain (TiN/CrN)×3), (5) nitrided CoCrMo with (TiN/CrN)×3 multilayer ((TiN/CrN)×3 duplex).

### Surface characterisation

Scanning Electron Microscopy observations of the cross-sections of the samples were carried out in a JEOL JSM-6510LV apparatus operated in backscattering mode and thickness of the nitrided layers and PAPVD coatings was determined. Surface roughness was determined by measuring the arithmetic mean roughness value Ra by means of AFM using a Quesant Instruments Corporation Q-Scope 250. The measurements were performed applying the square area of 50 μm using contact mode. The hardness and Young's modulus of the five experimental nitrided samples and then of the duplex composites were measured by means of the indentation method. To achieve this aim, the nano-hardness tester (NHT) made

by the Centre Suisse d'Electronique et de Microtechnique S.A was used. Measurements were carried out with the Berkovich indenter in a single cycle without stopping with under the following conditions: max depth = 250 nm, loading rate = 60 mN/min and unloading rate = 60 mN/min. To eliminate the influence of the substrate material on the result of the measurement of Young's modulus, the range of the indenter's penetration depth was limited to the value of  $g \leq 0.1 d$  ( $d$ -layer thickness). The hardness and Young's modulus were then determined by the Oliver and Pharr method.

### ***Chemical composition***

Investigations of the chemical composition of the experimental nitriding samples and then of the duplex composites were determined qualitatively by glow discharge-optical emission spectrometry (GDOES) method with the use of optical spectrometer Jobin Yvon JY10000RF and quantitatively using a X-ray microanalyzer (EDS- Noran Instruments) cooperating with a scanning electron microscope (Hitachi S2460N).

### ***Phase composition***

X-ray diffraction measurements were executed after nitriding process. These enabled to obtain information concerning to the phase composition of the nitrided sample. XRD was conducted on each sample using a Philips X'Pert diffractometer operated at 40 kV and 40 mA with  $\text{CuK}\alpha$  X-rays; the  $2\theta$  range for the specimens for this study was between  $30^\circ$  and  $80^\circ$ .

### ***Scratch test investigations***

The measurements of coating adhesion were carried out using the scratch-test method by means of a Revetest (CSEM) scratch-tester. The scratch indenter was a diamond stylus with a spherical tip having a radius of 200  $\mu\text{m}$ . For the 10 mm scratch length, the applied load was progressively increased from 0 to 100 N at a rate of 10 N/mm. Three scratch tests were performed for each sample and an average value the critical loads obtained. After the test, a critical load where failure occurred was determined by observation of the scratch track using an optical microscope Nikon MM40 with Panasonic KR222 video camera attached. The friction force and Acoustic Emission signals were recorded during the scratch

tests and later compared with the results of microscope observations of the scratches. The scratch resistant properties of the nitride layer and the coatings were then quantified in terms of the critical loads corresponding to the failure modes as defined as follows: first crack ( $L_{C0}$ ), beginning of the material removal ( $L_{C1}$ ), first breakthrough or lose of adhesion ( $L_{C2}$ ) and total material removal or worn out ( $L_{C3}$ ).

## RESULTS AND DISCUSSION

### Results of experimental nitriding processes

Results of investigations on samples nitriding with nitriding potentials  $p(N_2/H_2) = 1.0, 1.5, 2.0, 2.5$  and  $3.0$  are summarized in **Table 2**.

**Table 2. Results from experimental nitriding processes on CoCrMo alloy samples**  
Tabela 2. Właściwości warstw azotowanych uzyskanych na stopie CoCrMo

Sample No.	Nitriding potential	Thickness ( $\mu\text{m}$ )	Ra ( $\mu\text{m}$ )	H (GPa)	E (GPa)
CoCrMo	–	–	0.010	8.31	267
1	1	2.73	0.023	13.02	242
2	1.5	3.55	0.050	11.48	218
3	2	3.64	0.057	11.04	220
4	2.5	3.50	0.040	13.42	257
5	3	4.02	0.120	9.98	234

According to the results, the nitriding potential  $p(N_2/H_2) = 2.5$  was chosen. Although sample nitrided with nitriding potential  $p(N_2/H_2) = 3$  presents the higher thickness, its roughness is also higher ( $Ra = 0.120 \mu\text{m}$ ) and its mechanical properties are the lowest in comparison with the other samples. However, the sample nitrided using a nitriding potential  $p(N_2/H_2) = 2.5$  presents a thickness similar to samples 2 and 3 ( $3.5 \mu\text{m}$ ), but its roughness is the lowest from the five samples and presents the higher hardness.

### Configuration, chemical composition and parameters of the composites

**Fig. 1a** shows the cross-sectional SEM micrograph of CoCrMo alloy sample nitrided with  $p(N_2/H_2) = 2.5$ . This nitriding process in the Co-CrMo alloy produced a nitrided layer with a thickness of  $3.5 \mu\text{m}$ . The quantitative chemical composition over the nitrided layer was determined

by means of EDS analysis. The main elements and their concentrations on the nitrided layer were about 62% Cr, 14% Mo, 12% Co and 11% N (wt. %).

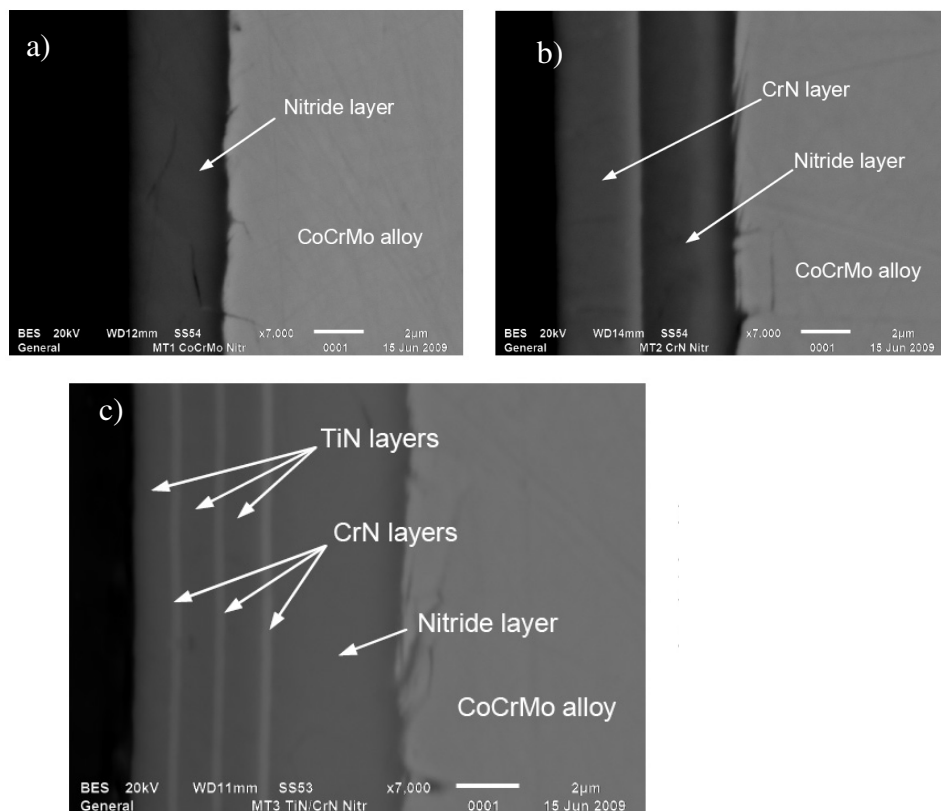


**Fig. 1. Cross-sectional SEM micrograph of: (a) CoCrMo nitrided with  $p(N_2/H_2)=2.5$ , (b) CrN duplex composite (nitrided layer + CrN PAPVD coating) and c)  $(TiN/CrN) \times 3$  duplex composite (nitrided layer +  $(TiN/CrN) \times 3$  PAPVD coating)**

Rys. 1. Obraz SEM przekroju warstw: a) azotowany stop CoCrMo dla  $p(N_2/H_2)=2.5$ , b) kompozyt warstwa azotowana + powłoka CrN, c) kompozyt warstwa azotowana powłoka  $(TiN/CrN) \times 3$

SEM micrograph of CrN duplex composite cross-section is shown in **Fig. 1b**. This image shows the PAPVD CrN layer followed by the nitride layer created during the duplex process in the CoCrMo sample. The thicknesses of these layers are 3.25 and 3.5  $\mu m$  respectively. The concentrations through the profile of the composite were 84% Cr, and 16% N

(wt. %) for the PAPVD CrN layer and then in the nitrided layer the content of chromium and nitrogen decreased to 62%, and 11% (wt. %) respectively and molybdenum and cobalt appeared with concentrations of 14 and 2% (wt. %) respectively.

**Fig. 1c** Shows cross-sectional SEM micrograph of duplex composite (TiN/CrN)×3. The configuration of this composite consisted of three TiN layers intercalated with three CrN layers with a thickness of 1 and 0.25 μm respectively, resulting in a 3.75 μm thickness multilayer PAPVD coating with followed by the 3.5 μm thickness nitrided layer created during the nitriding process. The chemical composition of each TiN inter-layer was about 74% Ti, 10%Cr and 16% N (wt%). For each CrN inter-layer the chemical composition was as follows: 70% Cr, 20% Ti and 10% N (wt. %). The elemental composition of the nitrided layer was 62.5% Cr, 20% Co, 14.5% Mo and 3% N (wt. %).

The SEM-EDS analyses for the CrN and (TiN/CrN)×3 PAPVD coatings applied to forged CoCrMo alloy samples without previous nitriding treatment (non-duplex), reveals that the configurations, chemical compositions and thicknesses of the PAPVD coatings are the same that for the PAPVD coatings in the duplex composites. The basic parameters and properties of the created duplex composites (nitrided layer/PAPVD coating), the PAPVD non-duplex coatings and nitrided CoCrMo alloy are summarized on **Table 3**.

**Table 3. Parameters and properties of the different conditions of CoCrMo alloy samples**

Tabela 3. Właściwości próbek stopu CoCrMo po różnych obróbkach powierzchniowych

Sample	Thickness (μm)	Roughness Ra (μm)	Hardness (GPa)	Young's Modulus (GPa)
CoCrMo		0.010	8.31	267
CoCrMo Nitrided	3.5	0.020	12.62	231
CrN duplex	3.25 CrN	0.100	19.64	286
	3.5 Nitrided layer			
CrN	3.25	0.100	19.40	283
(TiN/CrN)×3	3.75 (TiN/CrN)×3	0.165	26.23	400
duplex	3.5 Nitrided layer			
(TiN/CrN)×3	3.75	0.165	26.62	384



### 3 X-ray diffraction

Figure 2 shows the X-ray diffractograms of CoCrMo alloy before and after nitriding process. It can be observed that forged CoCrMo alloy untreated presents the FCC- $\alpha$  and HCP- $\epsilon$  cobalt parent structures. According to the Sage and Gillaud [L. 13, 14] model, the wt. % of HCP- $\epsilon$  phase on forged CoCrMo was 51%.

X-ray diffractograms revealed the presence of CrN phase in the nitrided layer. After nitriding process,  $\epsilon$  phase was inhibited and it disappears due to the high presence of N. A change is detected in (111) and (200) planes from parent  $\alpha$  structure with the appearance of CrN, in agreement with Refs [L. 1, 3].

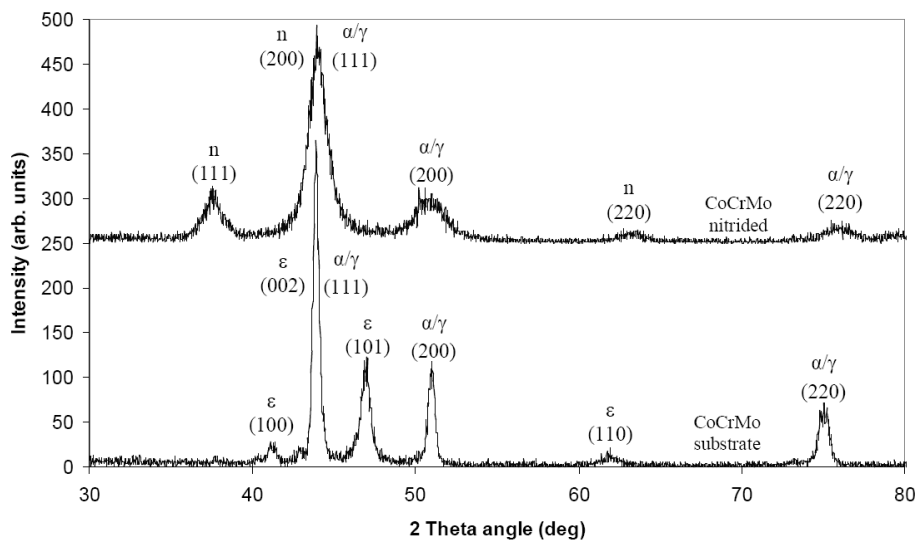


**Fig. 2. XRD results of: (a) CoCrMo alloy as-received and b) forged CoCrMo alloy after plasma nitriding with  $p(N_2/H_2) = 2.5$**

**Rys. 2.** Wyniki analizy XRD dla: a) stopu CoCrMo, b) stopu CoCrMo po azotowaniu plazmowym dla potencjału azotowego  $p(N_2/H_2)$  wynoszącego 2.5

### Scratch test

The scratch resistant properties of the nitride layer created in the nitriding forged CoCrMo alloy sample and the PAPVD coatings in forged CoCrMo alloy samples with and without previous nitriding treatment were quantified in terms of the critical loads corresponding to the failure modes mentioned before.

The failure events which took place during the scratch test on forged CoCrMo nitrided sample are shown in **Fig. 3**.

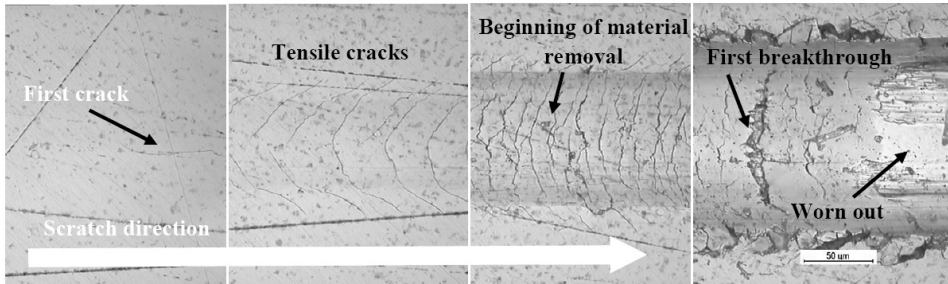


**Fig. 3. Main part of a scratch track on the nitride layer created on forged Co-CrMo alloy nitrided sample observed by optical microscopy at 500x magnification**

Rys. 3. Obrazy optyczne fragmentów rysy na powierzchni azotowanej na azotowanym stopie CoCrMo (scratchtest, powiększenie 50x)

At the beginning of the scratch test, the first crack occurred in the center of the scratch track parallel to the scratch direction at a load of 3.85 N ( $L_{C0}$ ). As the load continued to increase, the stylus ploughed in the nitride layer and tensile cracking occurs at 10 N. Cracks are transversally aligned to the scratch direction and the distance between cracks is in the range of 25–30  $\mu\text{m}$ . During further moving of the indenter and load rising, the distance between cracks decreased to 10  $\mu\text{m}$  and material was detached from the edge of the cracks across the scratch track when load reached 32 N and this event can be considered the beginning of the material removal ( $L_{C1}$ ). The substrate in the scratch track was exposed for the first time at 50.17 N. The occurrence of this failure event could be considered the first breakthrough or lose of adhesion at the critical load of  $L_{C2}$ . Finally, the nitride layer was worn out at a load of 54 N ( $L_{C3}$ ).

For the composite PAPVD (TiN/CrN) $\times$ 3 duplex, the main part of the scratch track produced during the scratch test is shown in **Fig. 4**. At an early stage of the scratch test, cracking took place in the porous surface of the PAPVD coating near to the edges of the scratch track parallel to the scratch direction when the load applied was increased to 9.40 N ( $L_{C0}$ ). As the load continued to rise, detachment of the TiN layer occurred at 32.27 N and the CrN coating was visible in some sections and also light tensile cracks appeared in the scratch track transversally to the scratch direction.

It can be considered the beginning of the material removal due to cohesive failure ( $L_{C1}$ ). Cracks became more pronounced with the increasing of load. When the load reached 68.30 N the coating was suddenly removed ( $L_{C3}$ ). Substrate was never visible until this load. It can be assumed that tensile cracks belongs to the CrN layer, because when the TiN layer sections are detached from the scratch track and the cracks remain in the CrN layer, it seems to be a cracked CrN coating with a layer of TiN smeared over.

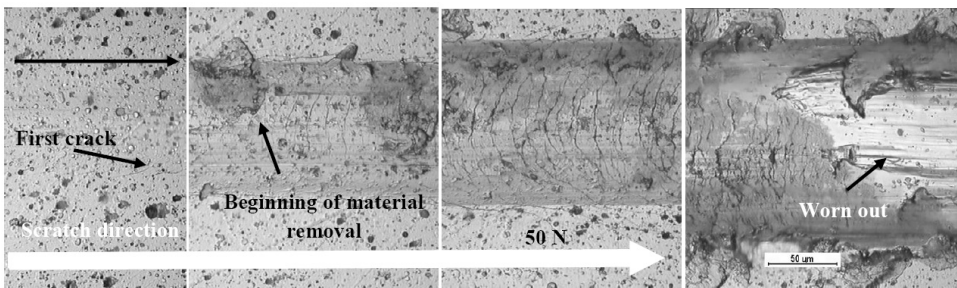


**Fig. 4. Main part of a scratch track on the composite (TiN/CrN)×3 duplex observed by optical microscopy at 500x magnification**

Rys. 4. Obrazy optyczne fragmentów rysy na powierzchni kompozytu warstwa azotowana powłoka / (TiN/CrN)×3 (scratchtest, powiększenie 50x)

**Fig. 5** shows the failure events on the composite (TiN/CrN)×3 non-duplex that occurred during the scratch test.

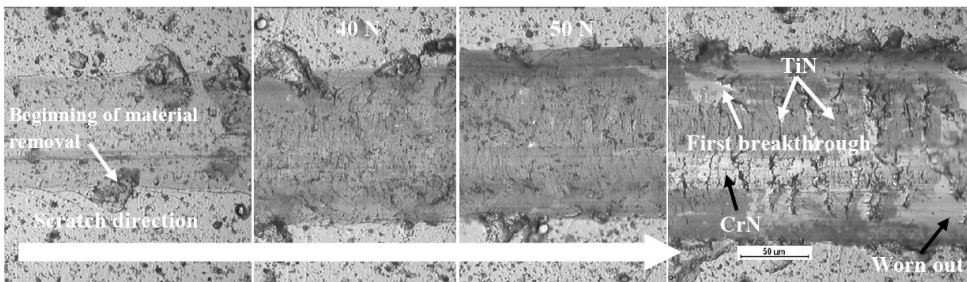


**Fig. 5. Main part of a scratch track on the composite (TiN/CrN)×3 non-duplex observed by optical microscopy at 500x magnification**

Rys. 5. Obrazy optyczne fragmentów rysy na powierzchni powłoki (TiN/CrN)×3 (scratchtest, powiększenie 50x)

In this sample, the first crack becomes visible in the edge of the scratch track parallel to the scratch direction when the load reached 7.96 N ( $L_{C0}$ ). With progressive loading, when load increased to 25 N, detachment of the TiN layer takes place in the edges of the scratch track and this event can be considered as the beginning of the material removal due to a cohesive failure ( $L_{C1}$ ). When load increased from 30 to 50 N, thinner transversal cracks appear in the scratch track with a distance between cracks from 3 to 5  $\mu\text{m}$ . When load increased to 55 N part from the TiN layer was removed and the substrate became visible through the cracks in the CrN layer. This event is the first break through where adhesion is lost ( $L_{C2}$ ). As the load continued to increase, the indenter ploughed in the coating and it was broken in 'islands' of multilayer coating in the scratch track. The coating was totally removed at a load of 58.5 N ( $L_{C3}$ ).

The scratch failure modes along the scratch tracks of the CrN duplex and non-duplex coatings were the same as those of the (TiN/CrN) $\times$ 3 duplex and non-duplex, only differentiated by the critical loads of occurrence. The mean values of critical loads corresponding to the different failure modes are summarized in **Table 4**.

**Table 4. Critical loads of the different CoCrMo conditions corresponding to the failure modes occurring during the scratch test.**

Tabela 4. Obciążenie krytyczne próbek stopu CoCrMo po różnych obróbkach powierzchniowych

Sample	Critical loads					
	$L_{C0}$ (N)	$L_{C1}$ (N)	$L_{C2}$ (N)	$L_{C3}$ (N)		
	First crack	Beginning of material removal	of re-through	First break-through	Worn out	
CoCrMo Ntrided	3.85	32.00		50.17	54.00	
CrN duplex	7.14	30.82		69.84	72.00	
CrN	5.50	22.48		57.40	60.00	
(TiN/CrN) $\times$ 3 duplex	9.40	32.27		N/A	68.30	
(TiN/CrN) $\times$ 3	7.96	12.90		55.00	58.50	

## CONCLUSIONS

Five experimental nitriding processes on CoCrMo orthopedic alloy were done to select an optimal nitriding potential. The CoCrMo alloy after the nitrided process presented a nitrided layer which chemical composition and structure that was evaluated by several analytical methods. CrN phase was detected in the nitride layer. Surface roughness, hardness and Young's Modulus of the substrate increased after plasma nitriding. PAPVD coatings were deposited on CoCrMo alloy with and without previous nitriding process and duplex composites (nitrided layer/PAPVD) were created. Results from scratch test shown that nitrided layer is harder and more brittle than the CoCrMo alloy substrate. Tensile cracks appeared transversally to the scratch track of the duplex composites.

The duplex technology applied to CoCrMo orthopedic alloy allows for:

- significant increase of the adhesion of the PAPVD coatings,
- improvement of the load carrying capacity of the CoCrMo orthopedic alloy.

On the basis of these investigations it can be stated that duplex composites and multilayer coatings are a promising alternative to solve the wear issue in orthopedic implants and it would be crucial to perform extensive investigations of these approaches on tribological devices under conditions similar to those in human body.

## REFERENCES

1. Çelik A., Bayrak Ö., Alsaran A., Kaymaz İ., Yetim A.F.: Surface and Coatings Technology, 202 (2008) 2433.
2. Wei R., Booker T., Rincon C., Arps J.: Surface and Coatings Technology, 186 (2004) 305.
3. Lanning B.R., Wei R.: Surface and Coatings Technology, 186 (2004) 314.
4. Fisher J., Hu X.Q., Tipper J.L., Stewart T.D., Williams S., Stone M.H., Davies C., Hatto P., Bolton J., Riley M., Hardaker C., Isaac G.H., Berry G., Ingham E.: Journal of Engineering in Medicine, 216 (2002) 219.
5. Fisher J., Hu X.Q., Stewart T.D., Williams S.: Journal of Materials Science: Materials in Medicine, 15 (2004) 225.
6. Walkowicz J., Smolik J., Tacikowski J.: Surface and Coatings Technology, 116–119 (1999) 370.
7. Smolik J., Walkowicz J., Tacikowski J.: Surface and Coatings Technology, 125 (2000) 134.

8. Smolik J., Gulde M., Walkowicz J., Suchanek J.: Surface and Coatings Technology, 180 (2004) 506.
9. He Y., Apachitei I., Zhou J., Walstock T., Duszczyk J.: Surface and Coatings Technology, 201 (2006) 2534.
10. Kamminga J.D., Alkemade P.F.A., Janssen G.C A.M.: Surface and Coatings Technology, 177–178 (2004) 284.
11. Hoy R., Kamminga J.D., Janssen G.C.A.M.: Surface and Coatings Technology, 200 (2006) 3856.
12. Chiba A., Kumagai K., Nomura N., Miyakawa S.: Acta Materialia, 55 (2007) 1309.
13. de J. Saldívar García A., Maní Medrano A., Salinas Rodríguez A.: Metallurgical and Materials Transactions A, 30 (1999) 1177.

**Recenzent:**

**Ewa KASPRZYCKA**

### **Streszczenie**

**Artykuł dotyczy oceny mechanicznych właściwości kompozytu warstwa azotowana/powłoka PVD utworzonego na stopie ortopedycznym CoCrMo stosowanym w aplikacjach biotribologicznych.**

**Przeprowadzono optymalizację procesu azotowania dla potencjału azotowego wynoszącego ( $p(N_2/H_2) = 1,0, 1,5, 2,0, 2,5$  i  $3,0$ ). Dla uzyskanych warstw azotowanych wykonano pomiary modułu elastyczności i twardości. W celu oceny grubości i jednorodności uzyskanych warstw wykonano obserwacje mikroskopowe (SEM) przekrojów poprzecznych. Zmiany chropowatości powierzchni zostały ocenione za pomocą stereometrycznych parametrów mierzonych z wykorzystaniem mikroskopii sił atomowych (AFM), natomiast zmiany składu fazowego za pomocą dyfrakcji rentgenowskiej (XRD). Uzyskane wyniki wskazały, że najkorzystniejsze właściwości warstwy wierzchniej uzyskano dla potencjału  $p(N_2/H_2)$ , wynoszącego 2,5.**

**Dokonano oceny wpływu azotowania podłoża na adhezję powłoki CrN oraz  $(TiN/CrN)_{x3}$  osadzanych metodą PAPVD z wykorzystaniem technik AFM, twardościomierza, SEM oraz scratchtestu.**

**Wykazano, że technologia duplex stosowana do ortopedycznego stopu CoCrMo pozwala na znaczne zwiększenie adhezji powłok PAPVD oraz poprawę jego właściwości przeciwzużyciowych.**